SCIENCE CHINA
Information Sciences

• MOOP •

December 2017, Vol. 60 123201:1–123201:9
doi: 10.1007/s11432-017-9261-1

Development of electric cart for improving walking ability — application of control theory to assistive technology

Jinhua SHE[1,2,3*], Yasuhiro OHYAMA[1*], Min WU[2,3*] & Hiroshi HASHIMOTO[4*]

[1]*School of Engineering, Tokyo University of Technology, Tokyo* 192-0982*, Japan;*
[2]*School of Automation, China University of Geosciences, Wuhan* 430074*, China;*
[3]*Hubei Key Laboratory of Advanced Control and Intelligent Automation for Complex Systems, Wuhan* 430074*, China;*
[4]*Master Program of Innovation for Design & Engineering, Advanced Institute of Industrial Technology, Tokyo* 140-0011*, Japan*

Received June 16, 2017; accepted October 23, 2017; published online November 9, 2017

Abstract This paper explains the development of an electric cart that helps the elderly maintain or improve their physical strength. Unlike commercially available ones, it has a pedal unit that provides some exercise for a user in training his lower limbs. An impedance model describes the feeling of pushing the pedals. The largest pedal load is determined based on a pedaling experiment. An H_∞ controller is designed for each of the largest pedal load and virtually no load. A control law, which is based on the concept of dynamic parallel distributed compensation, is designed using the rating of perceived exertion of a driver as a criterion to choose a pedal load between the largest and almost zero. Five university students and twelve elderly people participated experiments to verify the system design and the validity of the system.

Keywords aging, Borg's scale, dynamic parallel distributed compensation, electrical cart, H_∞ control, Karvonen formula, lower limbs, pedaling, rating of perceived exertion

Citation She J H, Ohyama Y, Wu M, et al. Development of electric cart for improving walking ability — application of control theory to assistive technology. Sci China Inf Sci, 2017, 60(12): 123201, doi: 10.1007/s11432-017-9261-1

1 Introduction

According to the definitions given by World Health Organization, aging rate is the ratio of people aged 65 and older to the population of a society. A country is considered as an aging society when the aging rate reaches 7%, an aged society if it reaches 14%, and a super-aged society if it is over 21% [1]. Japan became an aging society in 1970 (aging rate 7.1%), an aged society in 1994 (14.1%), and a super-aged society in 2007 (21.5%) [2]. The aging rate in Japan raised to 26.7% in 2015. Projections of the population with the current fertility rate show that 1 in 2.5 persons will be 65 and over, and 1 in 4 will be 75 and over by 2060. At that time, the total population will fall to 87 million, and the aging rate will be as high as about 40%.

* Corresponding author (email: she@stf.teu.ac.jp, ohyama@stf.teu.ac.jp, wumin@cug.edu.cn, hashimoto@aiit.ac.jp)

To handle this urgent problem, the Japanese government made the basic law on measures for the aging society as the basic framework of national measures for the aging society in 1995, and established the Aging Society Policy Council with the chairperson being the prime minister and all cabinet ministers being the members. General politics measurement for the aged society was formulated based on the basic law in 1996, and revised in 2001 and 2011. The government also tried to deal with the aging problem from scientific and technological aspects. In particular, the ministry of economy, trade, and industry and the ministry of health, labour, and welfare jointly designated four priority areas (lifting aids, mobility aids, toilets, monitoring systems for people with senile dementia) for scientific research to introduce robotics in nursing care of the elderly in 2012. The items in these areas were revised, and bathing was added into the list as a new area in 2014.

Many kinds of electric carts have been designed for the elderly to improve their mobility. However, those carts were designed solely as a means of transportation, and no consideration was given to an elderly person's need for physical exercise. To solve this problem, we designed a new-concept electric cart that not only helps people walk around, but also provides some exercise for their lower limbs. This paper presents a survey of our work on the development of the cart [3–5]. It rearranges the results we have obtained and provides explanations for them to ensure that a reader easily understands the flow of our study. Moreover, making the best use of MOOP (multimedia open online paper) allows us to provide a multimedia document, which contains experimental video clips, to deepen the understanding of our study. We originally designed a control system that not only produces a pedal load, but also provides an assist if the need arises. However, in order to keep the explanation simple, only the issue of how to generate a suitable pedal load is discussed in this paper. See [3, 4] for the issue regarding assistance.

2 Hardware design

The volume of lower-limb muscles greatly changes with aging. Statistics [6] show that, while the volume reaches the maximum during a person's twenties, it drops to 60% of the maximum in his seventies. Among walking muscles (lion muscle, gluteal muscle, front thigh muscle, hamstring muscle, calf muscle, shin muscle, and some others), lion muscle, front thigh muscle, shin muscle, and calf muscle become markedly weaker in later life. Considering that walking is one of the most important activity of daily life, we need to find measures to maintain or even increase the volume of those muscles.

Exploring all kinds of exercises, we found that cycling is an ideal exercise to work the walking muscles. Since front thigh muscle, calf muscle, and hamstring muscle are worked during pedaling down, and loin muscle, front thigh muscle, and shin muscle are worked during pedaling up, the walking muscles work during one circle of cycling. Therefore, we integrated a pedaling function into an electric cart, and developed a new-concept electric cart. Unlike the commercially available carts, this one has a pedal unit to exercise the walking muscles.

A commercially available three-wheeled electric cart, Everyday Type-S (Araco corporation, Japan; 330 W), was selected as the foundation of the system. The pedal unit contains two foot pedals and a pedal motor that generates a pedal load or assistance for a driver. It was designed with a special consideration to exercise. First, the load generated by the pedal motor is responsive to the road conditions. This provides a driver with a realistic driving experience. Second, electrical connection is used between pedals and drive wheels. This gives a designer great flexibility to adjust a pedal load.

The knowledge of ergonomics was made the best use for the installation of the pedal unit and the setup of the initial position of a seat so as to guarantee that pealing would be carried out in the optimal pedaling area (Figure 1).

An interface board (Figure 2) was assembled to handle the input and output signals. On the board, a PIC microcomputer chip (PIC16C74) was used to implement the functions of a D/A converter and a pulse counter, and a power operational amplifier (TA7272) was used to power control signals to the pedal and cart motors. Figure 3 shows a prototype of the new-concept electric cart.

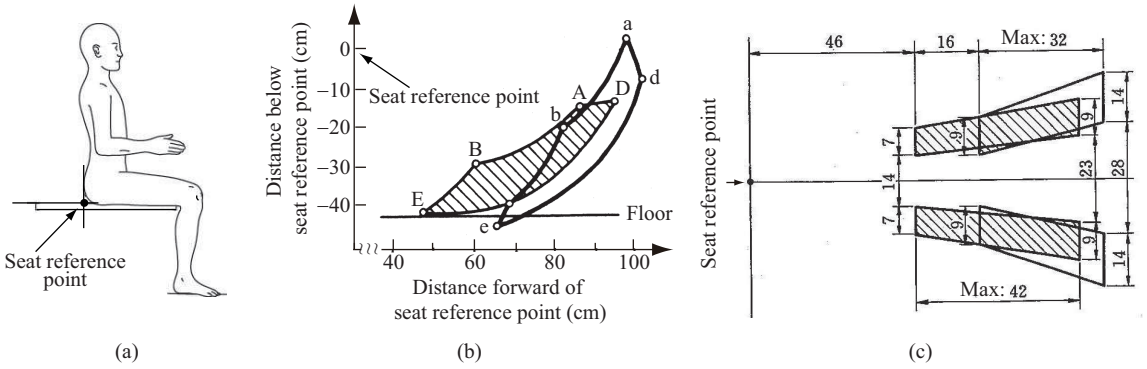

Figure 1 Optimal pedaling area. (a) Definition; (b) side view (upper case: heel; lower case: toe); (c) top view (unit: cm).

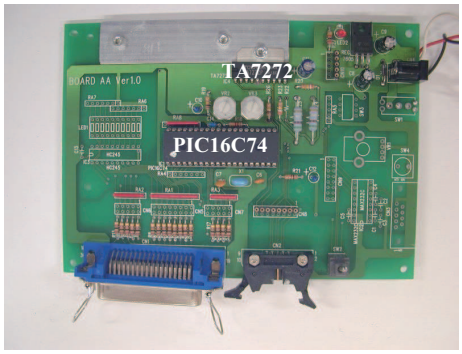

Figure 2 (Color online) Interface board.

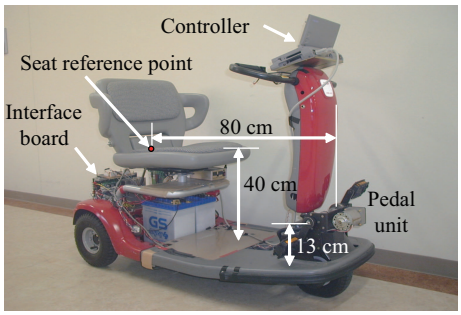

Figure 3 (Color online) Prototype electric cart.

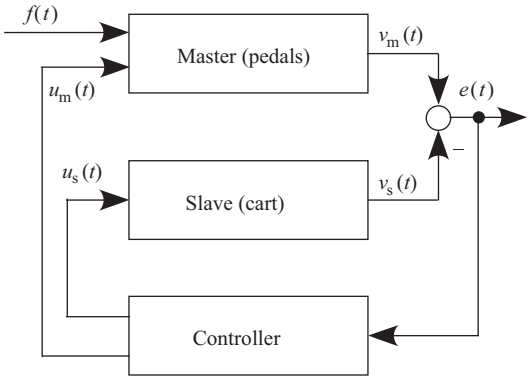

Figure 4 Bilateral master-slave cart control system.

3 Design of control system

The configuration of a bilateral master-slave control system (Figure 4) was employed for the design of a control system for the cart. The pedals are regarded as a master that generates a reference input for the cart, and the cart is regarded as a slave that tracks the input signal. Considering that a first-order plant is easy for a human to operate, we chose the pedaling speed, $v_{\mathrm{m}}(t)$, as the reference input. The rotational speed of the cart motor, $v_{\mathrm{s}}(t)$, tracks that of the pedal motor. In Figure 4, $f(t)$ is the pedaling force, $u_{\mathrm{m}}(t)$ and $u_{\mathrm{s}}(t)$ are the input voltages applied to the pedal and cart motors, respectively. So, the experience is very similar to riding a bicycle.

The heart rate of a driver is associated with a pedal load using the Karvonen formula to facilitate load

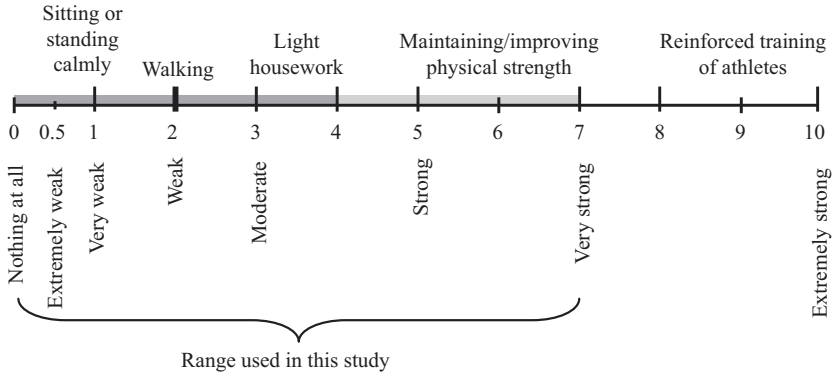

Figure 5 Borg CR10 scale.

selection. First, the rating of perceived exertion (RPE), r_{PE}, is calculated based on the formula [7]

$$r_{\mathrm{PE}} = \frac{\mathrm{HR} - \mathrm{HR_r}}{\mathrm{HR_m} - \mathrm{HR_r}} \times 100\%, \tag{1}$$

where HR is the current heart rate, $\mathrm{HR_r}$ is the heart rate at rest, and $\mathrm{HR_m}$ is the age-biased maximum heart rate:

$$\mathrm{HR_m} = 220 - \mathrm{age}. \tag{2}$$

Then, taking r_{PE} as one-tenth of the value on the Borg CR10 scale (Figure 5) [8] provides an estimate of the level of exertion for exercise, and it is used to select a pedal load. This is explained in the rest of this section.

A model of the master (pedals) is given by

$$\frac{\mathrm{d}v_{\mathrm{m}}(t)}{\mathrm{d}t} = A_{\mathrm{m}}v_{\mathrm{m}}(t) + B_{\mathrm{m}}u_{\mathrm{m}}(t) + B_{\mathrm{mf}}f(t), \tag{3}$$

where A_{m} is the system matrix of the master; and B_{mf} and B_{m} are the input matrices of the pedaling force and the voltage input applied to the pedal motor, respectively.

A model of the slave (cart) is

$$\begin{cases} \dfrac{\mathrm{d}v_{\mathrm{s}}(t)}{\mathrm{d}t} = A_{\mathrm{s}}(\Gamma)v_{\mathrm{s}}(t) + B_{\mathrm{s}}(\Gamma)u_{\mathrm{s}}(t), \\ A_{\mathrm{s}}(\Gamma) = A_{\mathrm{s0}} + \Phi\Gamma\Psi_A,\ B_{\mathrm{s}}(\Gamma) = B_{\mathrm{s0}} + \Phi\Gamma\Psi_B,\ \Gamma^{\mathrm{T}}\Gamma \leqslant I, \end{cases} \tag{4}$$

where $A_{\mathrm{s}}(\Gamma)$ is the system matrix of the slave, and $B_{\mathrm{s}}(\Gamma)$ is the input matrix of the voltage input applied to the cart motor. They are dependent on a driver's weight in the range $M = [45\ 100]$ kg, and are given by

$$\begin{cases} \Gamma(M) = \begin{bmatrix} \dfrac{A_{\mathrm{s}} - A_{\mathrm{s0}}}{\delta_A} & 0 \\ 0 & \dfrac{B_{\mathrm{s}} - B_{\mathrm{s0}}}{\delta_B} \end{bmatrix}, \\ A_{\mathrm{s0}} = \dfrac{A_{\mathrm{s}}|_{M=100} + A_{\mathrm{s}}|_{M=45}}{2},\ \delta_A = \dfrac{A_{\mathrm{s}}|_{M=100} - A_{\mathrm{s}}|_{M=45}}{2}, \\ B_{\mathrm{s0}} = \dfrac{B_{\mathrm{s}}|_{M=100} + B_{\mathrm{s}}|_{M=45}}{2},\ \delta_B = \dfrac{B_{\mathrm{s}}|_{M=100} - B_{\mathrm{s}}|_{M=45}}{2}. \end{cases} \tag{5}$$

An impedance model is introduced to describe the feeling of pushing the pedals:

$$\frac{\mathrm{d}v_{\mathrm{imp}}(t)}{\mathrm{d}t} = A_{\mathrm{imp}}v_{\mathrm{imp}}(t) + B_{\mathrm{imp}}f(t), \tag{6}$$

where $v_{\mathrm{imp}}(t)$ is the speed produced by model (6), A_{imp} is chosen to be A_{m}, and two values are selected for B_{imp} for two different modes of operation to suit the driver's physical condition: (1) strenuous mode

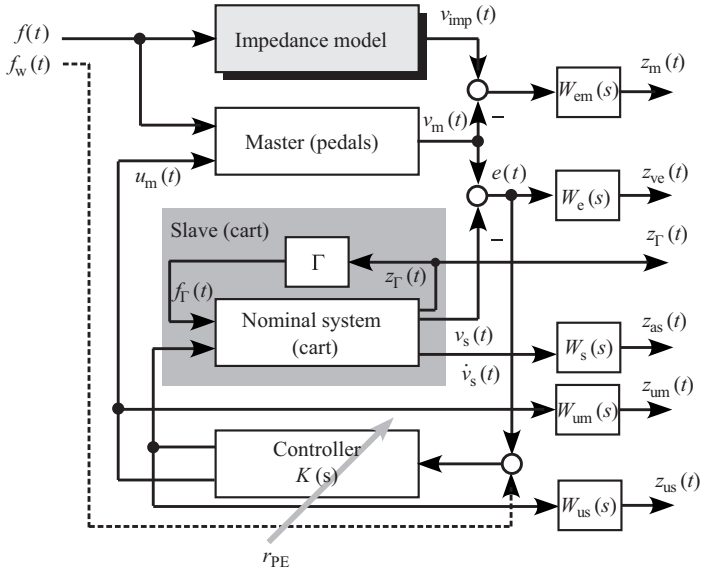

Figure 6 Block diagram used for design of cart control system.

($B^{\mathrm{S}}_{\mathrm{imp}}$), provides a pedaling load with its level as heavy as for walking; (2) neutral mode ($B^{\mathrm{N}}_{\mathrm{imp}}$), provides virtually no load.

$B^{\mathrm{S}}_{\mathrm{imp}}$ was determined by choosing a pedaling load that was corresponding to the level of exertion for walking, that is, $r_{\mathrm{PE}} = 20\%$ or 2 in the Borg CR10 scale. A pedaling experiment [4] yielded the maximum pushing force:

$$f_{\max} = 40 \text{ N}. \tag{7}$$

The design of the cart control system is divided into two steps. First, a controller is designed for each mode. Then, a controller for a pedal load in between strenuous and neutral modes is automatically generated using the concept of dynamic parallel distributed compensation. A brief description of the design is given below to make the paper self-contained. See [3, 4] for more information.

The H_∞ control method was used to design a controller for each of strenuous and neutral modes [3]. Let the exogenous inputs be $f(t)$ and $f_{\mathrm{w}}(t)$, where $f_{\mathrm{w}}(t)$ is a disturbance artificially added to the measured output channel to ease the design of an H_∞ controller. The controlled outputs are

(1) the weighted speed error between the impedance model and the pedals, $z_{\mathrm{m}}(t)$;

(2) the weighted speed error between the pedals and the wheels, $z_{\mathrm{ve}}(t)$;

(3) the weighted acceleration of the cart, $z_{\mathrm{as}}(t)$;

(4) the weighted voltage applied to the pedal motor, $z_{\mathrm{um}}(t)$;

(5) the weighted voltage applied to the cart motors, $z_{\mathrm{us}}(t)$.

In order to suppress $z_{\mathrm{m}}(t)$ and $z_{\mathrm{ve}}(t)$ at a low level at steady state, $W_{\mathrm{em}}(s)$ and $W_{\mathrm{e}}(s)$ are chosen to be low-pass filters. To keep the control voltages in an allowable range during the transient response, $W_{\mathrm{um}}(s)$ and $W_{\mathrm{us}}(s)$ are chosen to be high-pass filters. And to take into consideration of riding comfort, $W_{\mathrm{S}}(s)$ is chosen to be a low-pass filter based on ergonomics [9].

The small-gain theorem is used to guarantee the stability of the system, and the input and output of the uncertainty, $z_\Gamma(t)$ and $f_\Gamma(t)$, are added to the output and input vectors, respectively. As a result, letting the input be $w(t) = [f(t), f_\Gamma(t), f_{\mathrm{w}}(t)]^{\mathrm{T}}$ and the output be $z(t) = [z_{\mathrm{m}}(t), z_{\mathrm{ve}}(t), z_\Gamma(t), z_{\mathrm{as}}(t), z_{\mathrm{um}}(t), z_{\mathrm{us}}(t)]^{\mathrm{T}}$, we formulate the design problem as (Figure 6) *finding a controller* $K(s)$ *such that*

(1) *the cart control system is internally stable and*

(2) $\|G_{\mathrm{zw}}\|_\infty < 1$.

After we designed a controller for each mode, we conformed the validity of the controllers by experiments, which are explained in the next section. Then, we design a controller for a pedal load in between strenuous and neutral modes.

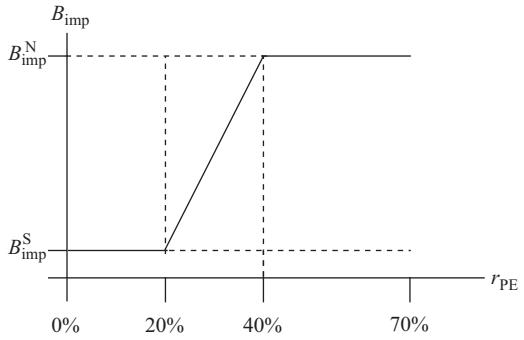

Figure 7 Relationship between pedal load and $r_{\rm PE}$ just before start of driving.

$r_{\rm PE}$ is measured when a driver rides on the cart. A pedal load is set by choosing the value of $B_{\rm imp}$ in (6) when $r_{\rm PE} < 70\%$, and the power to the cart is turned off when $r_{\rm PE} \geqslant 70\%$. $r_{\rm PE}$ is used as a criterion to select the pedal load as follows (Figure 7).

- Set the pedal load to the maximum (strenuous mode), that is, $B_{\rm imp} = B^{\rm S}_{\rm imp}$ when $r_{\rm PE} < 20\%$.
- Set the pedal load to a value suitable for the driver's health condition when $20\% \leqslant r_{\rm PE} \leqslant 40\%$,

$$B_{\rm imp} = \frac{40\% - r_{\rm PE}}{20\%} B^{\rm S}_{\rm imp} + \frac{r_{\rm PE} - 20\%}{20\%} B^{\rm N}_{\rm imp}. \tag{8}$$

- Set no pedal load (neutral mode), that is, $B_{\rm imp} = B^{\rm N}_{\rm imp}$ when $40\% < r_{\rm PE} < 70\%$.

Let the control inputs of the controllers for strenuous and neutral modes be $u^{\rm S}(t)$ and $u^{\rm N}(t)$ ($u(t) = [u_{\rm m}(t),\ u_{\rm s}(t)]^{\rm T}$), respectively. The control input based on the concept of dynamic parallel distributed compensation is given by

$$u(t) = \frac{40\% - r_{\rm PE}}{20\%} u^{\rm S}(t) + \frac{r_{\rm PE} - 20\%}{20\%} u^{\rm N}(t). \tag{9}$$

Clearly, the control input is generated based on those for strenuous and neutral modes, and the parameter $r_{\rm PE}$.

The stability of the control system for the control law (Eq. (9)) is guaranteed by the concept of dynamic parallel distributed compensation [4], which is explained below.

For each of strenuous and neutral modes, let $x(t) = [v_{\rm m}(t), v_{\rm s}(t)]^{\rm T}$, and the state of the controller be $x_{\rm ci}(t)$ [$i = {\rm S}$ (strenuous mode) or N (neutral mode)]. Then, the state space representation of the control system (Figure 4) is

$$\text{Master \& Slave}: \begin{cases} \dot{x}(t) = A_{\rm p}(\Gamma)x(t) + B_{\rm p}(\Gamma)u(t) + B_{\rm pf}f(t), \\ e(t) = C_{\rm p}x(t), \end{cases} \tag{10}$$

$$\text{Controller } (i = {\rm S}, {\rm N}): \begin{cases} \dot{x}_{\rm ci}(t) = A_{\rm ci}x_{\rm ci}(t) + B_{\rm ci}e(t), \\ u(t) = C_{\rm ci}x_{\rm ci}(t) + D_{\rm ci}e(t), \end{cases} \tag{11}$$

where

$$\begin{cases} A_{\rm p}(\Gamma) = \begin{bmatrix} A_{\rm m} & 0 \\ 0 & A_{\rm s0} \end{bmatrix} + \begin{bmatrix} 0 \\ \Phi \end{bmatrix} \Gamma \begin{bmatrix} 0 & \Psi_A \end{bmatrix} := A_{\rm p0} + \Phi_{\rm p}\Gamma\Psi_{{\rm p}A}, \\ B_{\rm p}(\Gamma) = \begin{bmatrix} B_{\rm m} & 0 \\ 0 & B_{\rm s0} \end{bmatrix} + \begin{bmatrix} 0 \\ \Phi \end{bmatrix} \Gamma \begin{bmatrix} 0 & \Psi_B \end{bmatrix} := B_{\rm p0} + \Phi_{\rm p}\Gamma\Psi_{{\rm p}B}, \\ B_{\rm pf} = \begin{bmatrix} B_{\rm mf} & 0 \end{bmatrix}^{\rm T}, \quad C_{\rm p} = \begin{bmatrix} 1 & -1 \end{bmatrix}. \end{cases}$$

The closed-loop system for each mode for $f(t) = 0$ is ($i = {\rm S}, {\rm N}$)

$$\begin{cases} \dot{\bar{x}}_i(t) = \bar{A}_i(\Gamma)\bar{x}_i(t), \\ \bar{x}_i(t) = \begin{bmatrix} x(t) \\ x_{\rm ci}(t) \end{bmatrix}, \ \bar{A}_i(\Gamma) := \begin{bmatrix} A_{\rm p}(\Gamma) + B_{\rm p}(\Gamma)D_{\rm ci}C_{\rm p} & B_{\rm p}(\Gamma)C_{\rm ci} \\ B_{\rm ci}C_{\rm p} & A_{\rm ci} \end{bmatrix}. \end{cases} \tag{12}$$

Write $\bar{A}_i(\Gamma)$ $(i = \mathrm{S}, \mathrm{N})$ as

$$\bar{A}_i(\Gamma) = \bar{A}_{i0} + \bar{\Phi}_i \Gamma \bar{\Psi}_i, \tag{13}$$

where

$$\bar{A}_{i0} = \begin{bmatrix} A_{\mathrm{p}0} + B_{\mathrm{p}0} D_{\mathrm{ci}} C_{\mathrm{p}} & B_{\mathrm{p}0} C_{\mathrm{ci}} \\ B_{\mathrm{ci}} C_{\mathrm{p}} & A_{\mathrm{ci}} \end{bmatrix}, \ \bar{\Phi}_i = [\Phi_{\mathrm{p}}^{\mathrm{T}}, \ 0^{\mathrm{T}}]^{\mathrm{T}}, \ \bar{\Psi}_i = [\Phi_{\mathrm{p}A} + \Phi_{\mathrm{p}B} D_{\mathrm{ci}} C_{\mathrm{p}}, \ \Phi_{\mathrm{p}B} C_{\mathrm{ci}}] .$$

Then, the stability of the closed-loop system, (12), for the control law, (9), is guaranteed if there exists a common symmetric positive-definite matrix $P = P^{\mathrm{T}} > 0$ such that

$$P\bar{A}_i(\Gamma) + A_i^{\mathrm{T}}(\Gamma) P < 0, \ i = \mathrm{S}, \mathrm{N} \tag{14}$$

hold. Or equivalently, if there exist a common symmetric positive-definite matrix $P = P^{\mathrm{T}} > 0$ and η_i such that

$$\begin{bmatrix} P\bar{A}_{i0} + \bar{A}_{i0}^{\mathrm{T}} + \eta_i \bar{\Psi}_i^{\mathrm{T}} \bar{\Psi}_i & P\bar{\Phi}_i \\ \bar{\Phi}_i^{\mathrm{T}} P & -\eta_i I \end{bmatrix} < 0, \ i = \mathrm{S}, \mathrm{N} \tag{15}$$

hold.

When a driver mounts the cart, a heart rate meter first measures his heart rate. Then, r_{PE} is calculated using (1), and a pedal load is set based on it.

4 Experiments and verification

In order to carry out experiments, first, we made an experimental plan and submitted it to the ethics committee at Tokyo University of Technology for assessment. After the plan was approved, we performed a serial experiments as follows.

(1) Select and verify the maximum pushing force (7) using an ergometer in a laboratory;

(2) Check if the controller works correctly (stability, the rules of pedal load selection, etc.) using an ergometer in the laboratory;

(3) Check if the cart control system works properly as designed and if the cart tracks the pedaling speed under different road conditions using the cart on different roads at the Hachioji campus of Tokyo University of Technology;

(4) Check if the cart control system selects a pedal load for a given r_{PE};

(5) Check if the cart control system selects a pedal load suited to a driver's RPE;

(6) Perform a questionnaire on the design of the pedal unit, the pedal load, and the control performance.

Five subjects, who were university students (ages: 21–25 years, sex: male), and twelve elderly people (ages: 65–83 years, sex: 4 male and 8 female) participated the experiments. The riding tests of the cart were carried out on a flat road, a 5° uphill road, and a 5° downhill road at the Hachioji campus of Tokyo University of Technology. The verification experiments showed that a pedaling load suited to each subject's condition was selected in every case. For example, the relationship between B_{p} and r_{PE} (Figure 8) shows that B_{p} increases (that is, the pedal load decreases) according to the designed rule as r_{PE} increases. The relationships between the average input voltage of the pedal motor and r_{PE}, and that between the average pushing force on pedals and r_{PE} for a flat road in the steady state are shown in Figure 9. It is clear that, as designed, the pedal load decreases as r_{PE} increases, and the applied voltage to the pedal motor increases as r_{PE} increases. The largest force, which is corresponding to strenuous mode was less than $f_{\max}$ (40 N). The speed response at steady state is shown in Figure 10. The variations in the applied voltage to the pedal motor and in the pedaling speed show the rhythm of pushing pedals. See other experimental results in the corresponding multimedia file.

All the experimental results confirmed the validity of the design of the pedal unit and the cart control system. More than 80% of the elderly people satisfied with the design and the control performance of the cart [4].

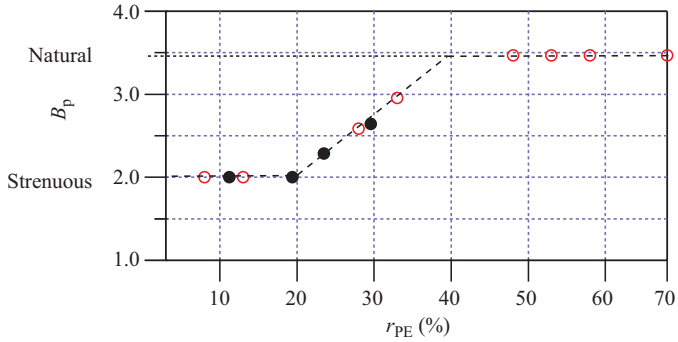

Figure 8 (Color online) Experimental results for relationship between B_p and r_{PE} [○: Subject 1 (21 years old); ●: Subject 2 (83 years old)].

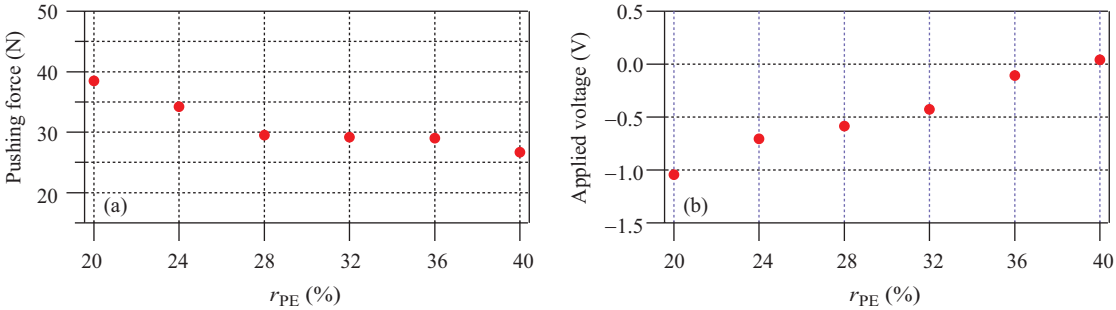

Figure 9 (Color online) Average pushing force/voltage of pedal motor vs. r_{PE} for flat road in steady state. (a) Average pushing force; (b) average input voltage of pedal motor.

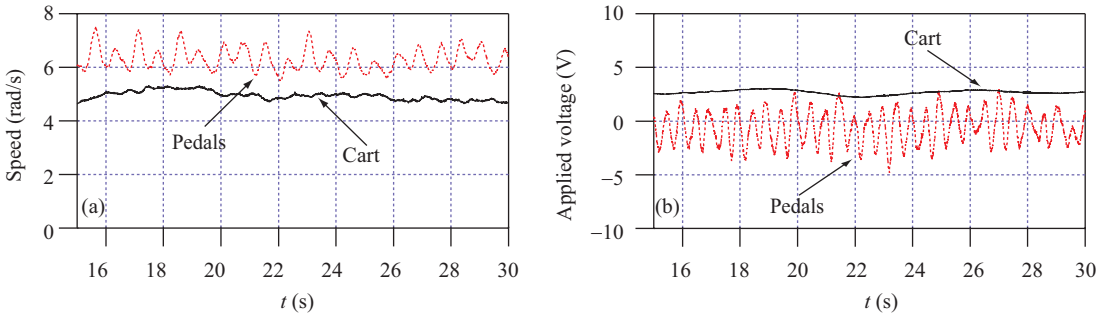

Figure 10 (Color online) Steady-state response for $r_{PE} = 20\%$ for flat road. (a) Pedal and cart speeds; (b) input voltages of pedal and cart motors.

5 Conclusion

This paper described a new-concept electric cart that has been developed to help the elderly maintain or improve their physical strength. The hardware design features ergonomical consideration for a pedal unit and the installation of the unit and seat. A pedal load was selected on the base of Borg's perceived exertion scale, the Karvonen formula, a pedaling experiment, and statistics on muscular degeneration. The cart control system, which guarantees the stability of the system and the suitable choice of a pedal load, was designed by incorporating the H_∞ control and the concept of dynamic parallel distributed compensation. Experiments involving young university students and elderly people demonstrate the validity of this cart control system.

Considering that people with lower-limb injuries are difficult to use this cart, we designed a bilaterally asymmetric pedaling machine [5], and planed to design a new electric cart so as to allow us to mount it on the cart.

On the other hand, even for the same pedaling load, there may have some differences in pedaling

motion (for example, the smoothness of pedaling motion and the movement of body centroid) between individuals. Those differences between young university students and the elderly may provide us some hints for the improvement of rehabilitation efficiency for the elderly. This issue will be examined in the future.

China became an aging society in 2000 (aging rate: 7.1%), and is accelerated heading for an aged society [10]. Many studies have been devoted to applying robotics to rehabilitation in the last few years [11, 12]. It is highly expected that the integration of robotics, medical care, information science, and material science will provide us a favorable environment for a society of health and longevity.

Acknowledgements This work was supported by Japan Society for the Promotion of Science (JSPS) KAKENHI (Grant Nos. 18560259, 26350673), and partially by JSPS KAKENHI (Grant No. 16H02883). This work was also supported by National Natural Science Foundation of China (Grant Nos. 61473313, 61210011), Hubei Provincial Natural Science Foundation of China (Grant No. 2015CFA010), and the 111 Project of China (Grant No. B17040).

Conflict of interest The authors declare that they have no conflict of interest.

Supporting information The supporting information is available online at info.scichina.com and link.springer.com. The supporting materials are published as submitted, without typesetting or editing. The responsibility for scientific accuracy and content remains entirely with the authors.

References

1 Okamura Y. Mainstreaming gender and aging in the SDGs. Ambassador and Deputy Representative of Japan to the United Nations at a Side Event to the High Level Political Forum, 2016. http://www.un.emb-japan.go.jp/jp/statements/okamura071316.html
2 Cabinet Office, Goverment of Japan. Annual Report on the Aging Society: 2016 (Summary) (in Japanese). 2017. http://www8.cao.go.jp/kourei/whitepaper/w-2013/zenbun/25pdf_index.html
3 She J, Ohyama Y, Kobayashi H. Master-slave electric cart control system for maintaining/improving physical strength. IEEE Trans Robotics, 2006, 22: 481–490
4 She J, Yokota S, Du E Y. Automatic heart-rate-based selection of pedal load and control system for electric cart. Mechatronics, 2013, 23: 279–288
5 She J, Wu F, Mita T, et al. Design of a new lower-limb rehabilitation machine. J Adv Comput Intel Intel Inform, 2017, 23: 409–416
6 Satoh M. Ningen Kougaku Kizyun Suuchi Suusiki Binran (Handbook of Ergonomic Standards, Statistics, and Numerical Formulae) (in Japanese). Tokyo: Gihodo Shuppan Company Limited, 1994
7 Hill D C, Ethans K D, Macleod D A, et al. Exercise stress testing in subacute stroke patients using a combined upper- and lower-limb ergometer. Arch Phys Med Rehabil, 2005, 86: 1860–1866
8 Borg G. Borg's Perceived Exertion and Pain Scales. Champaigne: Human Kinetics, 1998
9 Salvendy G. Handbook of Human Factors and Ergonomics. 2nd ed. New York: Willy, 1997
10 Japan International Cooperation Agency (JICA). JICA Report: Final Report on Information Collection and Confirmation Investigation of Aging Problem in China. 2014. http://open_jicareport.jica.go.jp/211/211/211_105_12153276.html
11 Peng L, Hou Z G, Peng L, et al. Robot assisted rehabilitation of the arm after stroke: prototype eesign and clinical evaluation. Sci China Inf Sci, 2017, 60: 073201
12 Hou Z, Zhao X, Cheng L, et al. Robot recent advances in rehabilitation robots and intelligent assistance systems (in Chinese). Acta Autom Sin, 2016, 42: 1765–1779